



Landslide Assessment Using Sentinel-1 SAR-C Interferometry Technique

Sudhir Kumar Chaturvedi†

Department of Aerospace Engineering, UPES, Dehradun-248007, India

†Corresponding author: Sudhir Kumar Chaturvedi, sudhir.chaturvedi@ddn.upes.ac.in

Nat. Env. & Poll. Tech.
Website: www.neptjournal.com

Received: 03-08-2021

Revised: 23-09-2021

Accepted: 20-10-2021

Key Words:

Landslide
Risk assessment
Human safety
SAR-C
Remote sensing

ABSTRACT

Landslides might remain unknown or unnoticed for a long time in various remote areas due to the unavailability of optical images caused by cloud persistence, which creates difficulties for civil protection rescue operations, and disaster management as well. Rapid crisis response for humanitarian and reconstruction operations in the affected area after such dangerous landslides is necessary. Thus, a rapid detection map is necessary to detect the affected area with damage grade and level for further investigation and human safety protocols. To detect landslide incidents, the unprecedented availability of Sentinel-1 SAR-C band images provides new solutions and better safety reports. In this study, we performed an efficient evaluation of Sentinel-1 SAR C band images before and after landslide incidents. This study provides a comprehensive evaluation based on the advanced space-borne remote sensing technology aiming at SAR products for rapid damage detection and analysis with respect to the interferometric coherence and intensity correlation. We presented the results of a pilot study on the Rudraprayag Uttarakhand massive landslide incident, which includes the different types, sizes, slope expositions, and human safety aspects. Our study and outcomes represent an updated method, which provides a solution for critical terrain rescue operations and an upgraded geomatics map that provides subsidence data with historical data with topographical statistics. Finally, an outlook into the Sentinel-1 SAR-C analysis demonstrates probable solutions to certain constraints, enabling global applicability of the proposed damage assessment methods with the improved accuracy from 50 to 60 % for the obtained temporal resolution datasets.

INTRODUCTION

Landslides are perhaps one of the most often occurring organic disasters around the world, constituting a severe hazard to human beings (human injury and loss of life) and infrastructure (destruction of construction/natural and ethnic heritage), and the organic atmosphere. Intense rain, earthquakes, and specified human pursuits are a number of the tripping facets of this landslide, which are shown in a variety of kinds and a broad selection of the volume of terrestrial materials (Tzouvaras et al. 2020). In an individual study, information from multiple detectors such as optical detectors, radar, UAVs, etc., was found efficiently to monitor the landslide. Recent studies show that interferometric SAR methods could satisfactorily be carried out in landslide observation, contributing to the understanding of its processes and dynamics, the mechanism of failure along with its mobility. In particular, two approaches of differential SAR interferometry (DInSAR) were employed for landslide investigation and observation as well as their outcome in comparison to earth tracking data demonstrated the viability of the technique in supplying information on the equilibrium of areas affected by slow-motion movements (Li et al. 2020). The more frequently used method of landslide distress tracking is Persistent Scattered Interferometry (PSI),

therefore various researchers have dealt with these specific situations. In other PSI scientific studies, information from various SAR assignments was united with each other as well as with present auxiliary data (geomorphological and geological, etc.) (Athos et al. 2020, Nguyen et al. 2020). The latest satellite SENTINAL-I assignment and available amount of data acquisition provided new inputs into the Landslide study, leading to a much more orderly watching of the aspects of uncertainty. Thus, research readings are completed introducing the principal elements of the interferometric dispensation of SENTINAL-I data, while in a respective Sentinel 1 information was manipulated as a way to upgrade inventory maps and also to monitor landslide activity. The recent study focuses on the claim of several processing methodologies: (a) interferogram generation, (b) assessment of the Digital Surface Model (DSM) earlier, and afterward the landslide function. Sentinel Application Platform (SNAP) was used in the current investigation, namely Sentinel-1 Toolbox (SITBX) created for the European Space Agency (ESA) by Array Systems Computing, German Space Centre (DLR), Brockmann Consult, and Ocean Data Lab.

In Fig. 1, a 3-dimensional topographic map depicts the landslide zone of Chandikadhar, Rudraprayag. As a result of enormous phase shifting of terrain geometry, the study

field, landslide description, and remote sensing survey of the landslide happened on October 21, 2019. The analysis area is Chandikadhar on the Kedarnath-Gaurikund Highway, Rudraprayag, Uttarakhand which is situated in north India (Fig. 1). The larger region is teeming with steep hillslopes and various inclinations that overpass stiff topographical angles in certain places (Vanama et al. 2020, Ahmed et al. 2020). The particle content is composed of three different geologic formations reflecting the elaborate geotectonic arrangement of the region. The study gives insight into the substantial successful software of the Advanced Differential Interferometric SAR (ADInSAR) procedure for landslide observation (Stankevich et al. 2020). For this reason, preprocessing along with post-processing suitability assessment methodologies were previously designed as essential components to verify the feasibility of the A-DInSAR ground deformation results for landslide observation. Specifically, preprocessing investigation is essential to value the structure of their A Differential Interferometry SAR technique for tracking previously mapped landslides as well as the finding of new subduction zones as a result of a previous discernibility chart (Meng et al. 2020). Meanwhile, post-processing analysis is vital to maintain consistency in assessing details such as landslide tracking. Differential Interferometry SAR techniques have advanced significantly, as evidenced by the development of SAR information assimilated by the ESA SENTINAL projects, which behave at advanced Spatial-Temporal settlement, and the growth of complex processing formulations (Table 1). So, the improvements from the DInSAR process necessitate a novel approach to assessing their probability

and constraints, which will be useful for local businesses such as environmental businesses and geological surveys in charge of large-scale landslide monitoring (Boni et al. 2020).

The procedure was developed and tested in the Rudraprayag area of Uttarakhand, in the Chandikadhar sector of the Kedarnath-Gaurikund Highway, using Sentinel-1 data from the ascending and descending modes from 2014 to 2020. The findings provide light on the complicated process' ability to detect monitor-able landslides, regions that require additional field data monitoring systems, and how to improve the representation of landslide movements by focusing on reliable measuring stations (Solari et al. 2019). The process may be used on almost any SAR platform, and it provides an instrument for connecting Sentinel 1 data for near real-time big landslide tracking that considers the benefits of A-DInSAR but also their limitations.

MATERIALS AND METHODS

Interferometric Coherence for Rapid Landslide

In the preceding section, the procedures involving Interferometric coherence and intensity correlation are explained. The difference in coherence or intensity significance values before and after the disaster to detect the shift, i.e., the damage caused by the disaster is analyzed. For instance, the coherence is first approximated using the pre-event InSAR pair (t_x and t_y). This allows for the identification of artificially commanded sites and areas, which are distinguished by their considerably large coherence values in comparison to

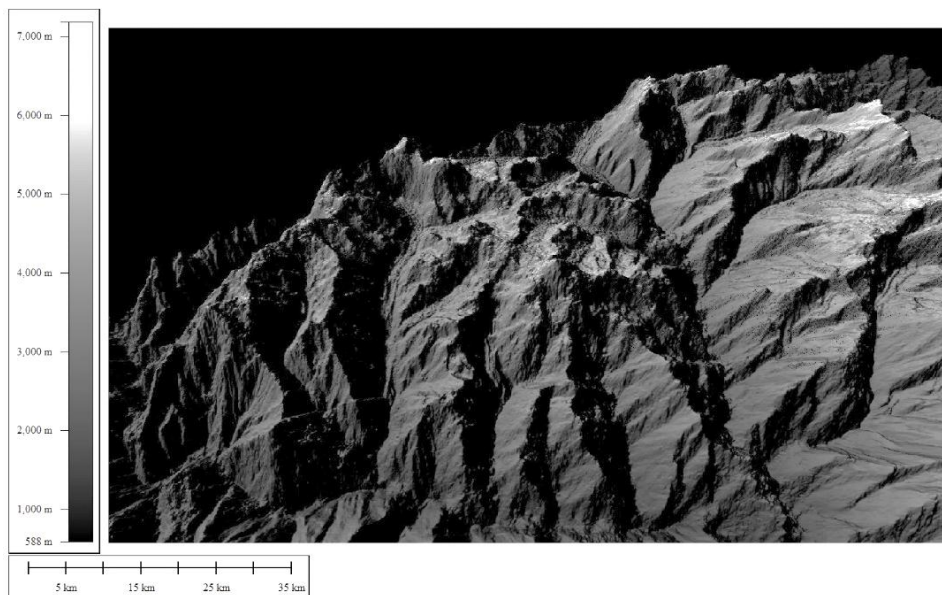


Fig. 1: Landslide zone 3-dimensional topographic map generated from Cartosat-1 DEM (30.401856° N, 78.930994° E).

Table 1: Advantages of the damage assessment approach.

Method (General)	Advantages	Achieved Accuracies
Interferometric coherence	Enables better differentiation of slightly damaged and undamaged areas.	45%–49%
SAR intensity correlation	More sensitive to larger changes (stronger damages) on the ground. Provides still useful information at spatial and temporal baselines, which are too large for useful coherence application.	41%–55%
Combination of coherence and intensity correlation (and SAR backscatter)	Strong increase of the damage assessment accuracy compared to the application of only interferometric coherence or intensity correlation, respectively.	52%–60%
Use of additional data (e.g., optical imagery and GIS data)	An additional increase in the damage assessment accuracy (compared to Section 3.3). Presentation of the damage level at meaningful distribution (e.g., city parcel boundaries, building blocks, etc.) enables the generation of damage maps more suited to the user.	77%–88%

stagnated areas. The coherence of the co-event InSAR sets t_y and t_z is computed in the second step. The phase-shifting concept is used to measure damage (Bakon et al. 2020, Luti et.al. 2020, Motagh et al. 2020)

The technique’s concept is that events that cause structural damage, such as earthquakes, hurricanes, flooding, and other natural disasters, dominate the de-correlation of their interferometric coherence. As a result, it is possible to specify the disaster related to the event by measuring the pre-disaster coherence as well as the co-disaster coherence. Hence, only areas controlled by urban structures could be assessed for damage (Nhu et al. 2020, Zhang et al. 2019)

$$ND = \frac{X_{pre} - X_{co}}{X_{pre} + X_{co}} \dots(1)$$

X_{pre} represents the Pre-disaster SAR image set (t_x and t_y in Fig. 3) along with X_{co} symbolizing a pre and a post-disaster image set containing the event (t_y and t_z in Fig. 3). The normalized differences approach could be applied to both, the interferometry coherence ND_γ and also the intensity significance ND_ρ :

$$ND_\gamma = \frac{\gamma_{pre} - \gamma_{co}}{\gamma_{pre} + \gamma_{co}} \dots(2)$$

$$ND_\rho = \frac{\rho_{pre} - \rho_{co}}{\rho_{pre} + \rho_{co}} \dots(3)$$

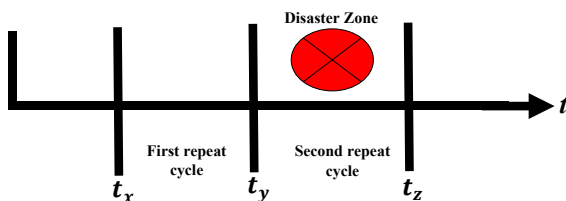


Fig. 2: The damage assessment interferometry Coherence method and SAR intensity correlation in which two image areas were acquired before the occasion which is t_x and t_y with respect to at least one SAR acquisition soon after the disaster at t_z condition.

The selection and conclusion of a practical threshold to distinguish between damaged and undamaged structures or to determine unique damage class ranges is critical for all change detection techniques (Intrieri et al. 2020). It is concentrated on the use of interferometric coherence for damage evaluation and introduced a coherence change index τ , at which γ_{pre} is the coherence of this pre-disaster SAR image set (t_x and t_y in Fig. 3) and γ_{co} is your coherence calculated by a pre-plus a post-disaster image set for the event (t_y and t_z in Fig. 3):

$$\tau = \frac{\gamma_{pre}}{\gamma_{co}} \dots(4)$$

Every pixel in this field of interest has its coherence indicator calculated. In contrast to the first SAR imaging, one must consider that the coherence is calculated over a few spaces, resulting in a loss in spatial resolution. Damage assessment, on the other hand, is far more practicable at coarser models such as administrative boundaries or building codes than at that pixel worth. The minimum dimensions of this ground target to be studied throughout the damage evaluation process are predetermined by the spatial resolution of this SAR detector. It can range from single buildings to the availability of very high spatial resolution SAR data if data from SAR detectors with lower plasma resolution can be found (Table 2). (Wasowski & Pisano 2020, Hayati et al. 2019, Shang et al. 2020). Another process of disaster management systems was also discussed by Chaturvedi et al. (2016), Srivastava et al. (2017), Chaturvedi (2019), and Guven et al. (2018) in terms of modeling and simulations of its parameters in deep, intermediate, and shallower water regions. The noise reduction techniques in RADAR datasets have been developed by Sood et al. (2018).

Datasets and Methodology

The methodology of interferogram for the calculation of ground displacement is a procedure that has just been ac-

Table 2: Synthetic Aperture Radar (SAR) missions relevant to this damage assessment study.

SAR Mission	Launch	Out of Service	Band *	Spatial Resolution (Azimuth and Ground Range) (m) **	Repeat Cycle (Days)
ERS-1	1991	2000	C	30	35
ERS-2	1995	2011	C	30	35
ENVISAT/ASAR	2002	2012	C	30	35
Radarsat-1	1995	2013	C	8-100	24
Radarsat-2	2007		C	2-160	24
Sentinel-1	2014		C	5-40	12 (6 ***)
J-ERS-1	1992	1998	L	18	46
ALOS/PALSAR	2006	2011	L	10-100	44
COSMO-SkyMed	2007		X	1-30	16 (4 ****)
TerraSAR-X	2007		X	1-40	11

tualized in the estimation of ground deformation in zones affected by a seismic tremor with massive consequences. Along these lines, this work, it was analyzed the particular technique in planning ground deformation after the event of a landslide. Specifically, the interferogram situation was done with the point of inspecting interferometric borders in territories exposed to distortion. In this manner, eight Sentinel-1 interferometric wide-area mode images were obtained and thus four sets were handled in this experiment. Correlation of interferometric DSM concerning assistance

variations after the landslide, two interferometric phase maps were made and, in this manner, looked at one another. Interferometric phase map precision has just been tried in a few examinations using information from various missions. In the particular work, 30 interferometric wide-area mode Sentinel-1 images, covering the territory of Chandikadhar, Rudraprayag, were acquired to deliver two interferometric phase-shifting maps, one preceding and another after the slide. It references that during the precise technique, it was viewed as the way that the ideal opposite benchmark for in-

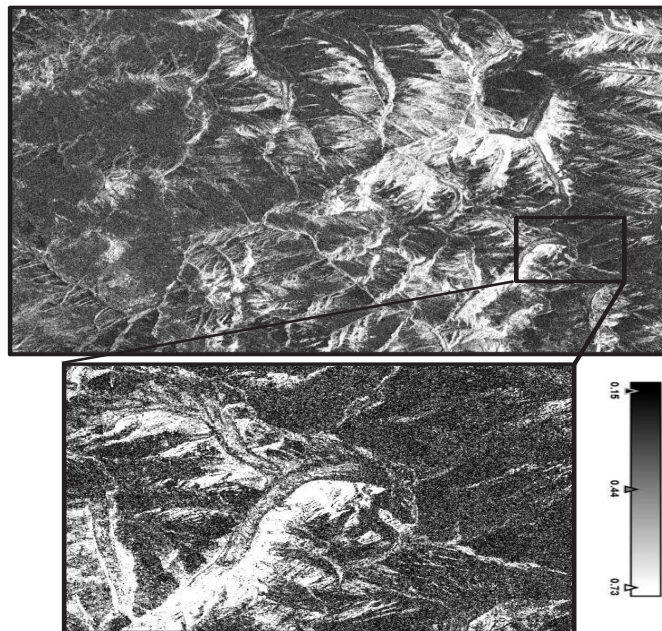


Fig. 3: Intensity interferogram VV SAR-C band landslide zone image analysis results from 12th October 2019 to 24th October 2019 (30.401856° N, 78.930994° E).

terferometric phase-shifting must be in the range somewhere in the range of 520m and 700m.

RESULTS AND DISCUSSION

Interferogram phase regarding four interferometric sets, made by four Sentinel-1 interferometric wide-area mode images before the landslide and other four images after the case, were acquired and held utilizing the interferometric process. In the formed interferogram, a change of colors was introduced at the landslide territory, which didn't show up in a similar zone before the event of the landslide. . In a similar article, a large number of dynamic landslides were identified using a relating technique, demonstrating the utility of Sentinel-1 data for landslide investigation and observation. The outputs illustrate the color shift that occurs within the boundary lines that denote the landslide's bounds. It shows that the landslide's limitations were calculated using spatial data and that they have a startling level of precision as a result. Fig. 3 shows the intensity interferogram VV SAR-C band landslide zone image analysis from Chandikadhar, Rudraprayag area on October 12th, 2019. Moreover, to confirm the precision of the outcomes, another interferogram was produced utilizing information before the slide, in which no shading adjustment happened at the terrain structure of the slide. Specifically, outputs show the created interferogram of Sentinel-1 rising information, while comprising the originated interferogram of handling Sentinel-1 information. The subsequent meth-

odology, Correlation of interferometric DSM, was used to examine two interferometric DSM and was used to examine elevation changes after the slide. To build elevation models based on the correlation of the two interferometric DSMs, six segments were drawn diagonally to the center of the slide. For Counterbalancing, the rapid landslide phase interferogram procedure requires two Sentinel-1 Ground Range Detected (GRD) information, which has as of now preprocessed and registered. The benefit of the particular procedure is that no stage data is required, so no climatic segment is recollected for conclusive outcomes. Fig. 4 is the depiction of rapid landslide phase interferogram VV output from 12th October 2019 to 24th October 2019 (30.401856° N, 78.930994° E).

The handling was updated by setting the matrix azimuth and range dividing values in pixels, which correspond to similar boundaries. Certain parts of the slide, particularly in the uppermost reaches, appeared to move more in accordance with the principal body of the slide. The precise process necessitates some consistent focus to differentiate and measurements for the rest territory's progressions. The progressions in the impacted region of the slide were gigantic to the point where the calculation couldn't figure out how to discover any steady spot to measure the movement effectively.

CONCLUSION

After a major disaster, quick emergency response is critical to support, humanitarian, and rescue efforts in the impacted

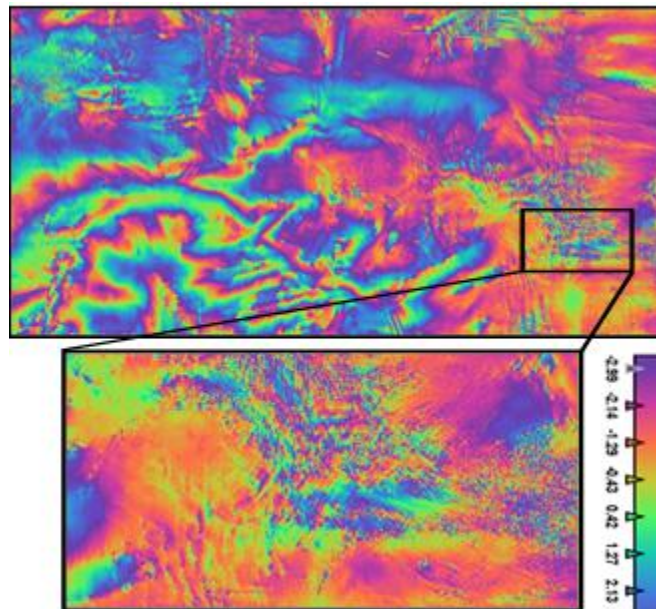


Fig. 4: Rapid landslide phase interferogram VV output from 12th October 2019 to 24th October 2019 (30.401856° N, 78.930994° E).

area. Quick disaster planning provides important information about the affected area, including the evaluation and type of disaster. Because of its quick response and ability to observe large areas at a low cost, satellite distant detection is crucial in disaster evaluation. As a result, SAR sensors are huge and provide useful imagery in a shorter period than optical sensors. A complete inspection of disaster assessment methods utilizing multi-temporal SAR methodology, for example, interferometric analysis and SAR detection were introduced. In opposed to this, both interferometric analyses, just as the SAR detection shows a decline of their qualities with expanding disaster level, as the period of the compound SAR backscatter fluctuations because of disaster at the ground. In this manner, the interferogram process is more capable to recognize lower disaster levels just as to even more likely separate between marginal disaster and massively affected structures. Unchanged regions have higher rationality estimation over a longer period at longer SAR frequencies, such as the L-band, as opposed to the shorter C or X-band, which also leads to better clarity in distinguishing between disaster and intact zones, and thus to better separation of both. This methodology can be divided into two categories: the first is the requirement for a rapid, relevant disaster evaluation methodology with high accuracy, and the second is the availability of any rate for two predicable SAR images acquired in a matter of seconds before the event at a similar image geometry as the post-calamity SAR assessments. The use of alternative datasets to pre and post-processed SAR images could be a potential answer for increasing the accuracy of disaster evaluation. For example, the accuracy of disaster evaluation strategies was increased from about 50% to 60% by combining radar and optical image datasets (because of just SAR assessments relationship and additionally coherence rate). As a result, a geodatabase comprising important GIS information and ongoing recalculation might be built up for any key territory of intrigue exposed to certain hazards. To evaluate the change location, i.e., disaster detection, a few strategies have been considered. Different investigations make use of more distinct alteration location approaches, such as the neural system-dependent system. The most important and advanced aspect of disaster assessment is identifying the disaster and determining its magnitude. As a result, space-based remote sensing applications are more precise and useful for any rapid detection of landslide-affected zones, resulting in improved safety and human rescue operations.

ACKNOWLEDGEMENT

The authors would like to thank UPES Dehradun for facilitating the space to carry out the research work. Corresponding author thanks Mr. Saikat Banerjee and Sourav Basu

of CubicX India for the great support in terms of the data processing and analysis.

REFERENCES

- Ahmed, B., Rahman, M.S., Sammonds, P., Islam, R. and Uddin, K. 2020. Application of geospatial technologies in developing a dynamic landslide early warning system in a humanitarian context: The Rohingya refugee crisis in Cox's Bazar, Bangladesh. *Geomat. Nat. Hazards Risk*, 11(1): 446-468.
- Athos, A., Lysandrou, V. and Hadjimitsis, G. 2020. Earth observation contribution to cultural heritage disaster risk management: A case study of Eastern Mediterranean open-air archaeological monuments and site. *Remote Sens.*, 12 (08): 60-67.
- Bakon, M., Czikhardt, R., Papco, J., Barlak, J., Rovnak, M., Adamisin, P. and Perissin, D. 2020. remotIO: A Sentinel-1 multi-temporal InSAR infrastructure monitoring service with automatic updates and data mining capabilities. *Remote Sens.*, 12(11): 515-525.
- Boni, R., Bordoni, M., Vivaldi, V., Troisi, C., Tararbra, M., Lanteri, L., Zucca F. and Meisina C. 2020. Assessment of the Sentinel-1 based ground motion data feasibility for large scale landslide monitoring. *Landslides*, 17: 2287-2299.
- Chaturvedi, S.K., Guven, U. and Srivastava, P.K. 2016. Measurement of tsunami wave Eigenvalues in deep, intermediate, and shallower regions. *Curr. Sci.*, 110(12): 750-756.
- Chaturvedi, S.K. 2019. A case study of the tsunami detection system and ocean wave imaging mechanism using radar. *J. Ocean Eng. Sci.*, 04(03): 203-210.
- Guven, U., Chaturvedi, S.K. and Srivastava, P.K. 2018. Measurement and validation of tsunami Eigenvalues for the various water wave conditions. *J. Ocean Eng. Sci.*, 05(01): 41-54.
- Hayati N., Wolfgang N. and Sadarviana V. 2019. Ground deformation in the cilito landslides area was revealed by multi-temporal InSAR. *Geosciences*, 10(5): 11-19
- Intrieri, E., Frodella, W., Raspini, F., Bardi, F. and Tofani, V. 2020. Using satellite interferometry to infer landslide sliding surface depth and geometry. *Remote Sens.*, 12(9): 4-12.
- Li, M., Zhang, L., Ding, C., Li, W. and Luo, H. 2020. Retrieval of historical surface displacements of the Baige landslide from time-series SAR observations for retrospective analysis of the collapse event. *Remote Sens. Environ.*, 240: 55-60.
- Luti, T., Segoni, T.S., Catani, F., Munafò, M. and Casagly, N. 2020. Integration of remotely sensed soil sealing data in landslide susceptibility mapping. *Remote Sens.*, 12(9): 55-60.
- Meng, Q., Confuorto, P., Peng, Y., Raspini, F., Bianchini, S., Han, S., Liu, H. and Casagly, N. 2020. Regional recognition and classification of active loess landslides using two-dimensional deformation derived from Sentinel-1 interferometric radar data. *Remote Sens.*, 12(10): 54.
- Motagh, M., Roessner, S., Akbari, B., Behling, R., Vassileva, M.S., Haghighi, M.H. and Ulrich-Wetzell, H. 2020. Landslides Triggered by 2019 Extreme Rainfall and Flood Events in Iran: Results from Satellite Remote Sensing and Field Survey. In EGU General Assembly Conference Abstracts, p. 10715.
- Nguyen, V., Yariyan, P., Amir, M., Tran, A.D., Pham, T.D., Do, M.P., Ngo, P., Nhu, V., Long, N.Q. and Bui D. 2020. A new modeling approach for spatial prediction of flash floods with biogeography optimized CHAID tree ensemble and remote sensing data. *Remote Sens.*, 12(9): 61.
- Nhu, V., Mohammadi, A., Shahabi, H., Bin Ahmad, B., Al-Ansari, N., Shirzadi, A., Clague, J., Jaafari A., Chen, W. and Nguyen H. 2020. Landslide susceptibility mapping using machine learning algorithms and remote sensing data in a tropical environment. *Int. J. Environ. Res. Public Health*, 17(14): 101.

- Shang, J., Jiali, J., Liu, J., Poncos, V., Geng, X., Qian, B., Chen, Q. and Dong, T. 2020. Detection of crop seeding and harvest through analysis of time-series Sentinel-1 Interferometric SAR data. *Remote Sens.*, 12(10): 121.
- Srivastava, P.K., Guven, U. and Chaturvedi, S.K. 2017. A brief review on tsunami early warning detection using the BPR approach and post-analysis by SAR satellite dataset. *J. Ocean Eng. Sci.*, 02(02): 83-89
- Solari, L., Bianchini, S., Franceschini, R., Barra, A., Monserrat, O., Thuegaz, P., Bertolo, D., Crosetto, M. and Catani, F. 2019. Satellite interferometric data for landslide intensity evaluation in mountainous regions. *Int. J. Appl. Earth Observ. Geoinform.*, 6: 87
- Sood, A., Shah, A. and Katyay, A. 2018. MATLAB-based graphical user interface development of RADAR with the implementation of noise under various brands. *Lect. Notes Mech. Eng.*, 11: 69-76.
- Stankevich, S., Piestova, I., Kozlova, A., Titarenko, O. and Singh, S.K. 2020. Satellite Radar Interferometry Processing and Elevation Change Analysis for Geoenvironmental Hazard Assessment. In Srivastava, P.K., Singh, S.K., Mohanty, U.C. and Murty, T. (eds.), *Techniques for Disaster Risk Management and Mitigation*, John Wiley & Sons, New York, pp. 125-139
- Tzouvaras, M., Danezis, C. and Hadjimitsis, D.G. 2020. Small scale landslide detection using Sentinel-1 Interferometric SAR coherence. *Remote Sens.*, 12(10): 1560-1567
- Vanama, V.S.K., Mandal, D. and Rao, Y.S. 2020. GEE4FLOOD: rapid mapping of flood areas using temporal Sentinel-1 SAR images with Google Earth Engine cloud platform. *J. Appl. Remote Sens.*, 14(3): 414-425.
- Wasowski, J. and Pisano, L. 2020. Long-term InSAR, borehole inclinometer, and rainfall records provide insight into the mechanism and activity patterns of an extremely slow urbanized landslide. *Landslides*, 17(2): 445-457.
- Zhang, C., Liu, Y., Gao, P., Chen, W., Li, H., Hou, Y., Nuremanguli, T. and Ma, H. 2019. Landslide mapping with remote sensing: challenges and opportunities. *Int. J. Remote Sens.*, 41(4): 1555-1581.